

# Dynamic analysis of single-degree-of-freedom systems (DYANAS): A graphical user interface for OpenSees

Georgios Baltzopoulos<sup>a,\*</sup>, Roberto Baraschino<sup>a,b</sup>, Iunio Iervolino<sup>a</sup>, Dimitrios Vamvatsikos<sup>b</sup>

<sup>a</sup> University of Naples Federico II, Department of Structures for Engineering and Architecture, Via Claudio 21, Naples, Italy

<sup>b</sup> National Technical University of Athens, Department of Civil Engineering, Heroon Polytechniou 9, Athens, Greece

## ARTICLE INFO

### Keywords:

Performance-based earthquake engineering  
Pushover analysis  
Incremental dynamic analysis  
Multiple-stripe analysis  
Cloud method

## ABSTRACT

Non-linear dynamic response of SDOF systems enjoys widespread application in earthquake engineering, sometimes as a testing ground for cumbersome analytical procedures, but often as a direct proxy of first-mode-dominated structures, within the family of simplified, pushover-based methods for seismic structural assessment and/or design. This article presents DYANAS, a MATHWORKS-MATLAB<sup>®</sup>-based graphical user interface that uses the OpenSees finite element platform to perform nonlinear dynamic analysis of single-degree-of-freedom (SDOF) oscillators. The scope of this open-source, freely distributed software is to serve as a tool for earthquake engineering research. The main advantages offered by the DYANAS interface are ease in the definition of the required analysis parameters and corresponding seismic input, efficient execution of the analyses themselves and availability of a suite of convenient, in-built post-processing tools for the management and organization of the structural responses. The types of dynamic analysis frameworks supported are incremental, multiple-stripe and cloud. Simultaneous consideration of pairs of uncoupled dynamic systems gives the possibility for intensity measures to refer to bidirectional ground motion. In the paper, an outline of the types of dynamic analysis frameworks typically used in performance-based earthquake engineering is provided, followed by a detailed description of the software and its capabilities, that include an array of post-processing tools. In order to properly place this software tool within its natural performance-based earthquake engineering habitat, some example applications are provided at the end of the paper.

## 1. Introduction

Earthquake engineering sees widespread usage of simple structural systems, such as single-degree-of-freedom (SDOF) yielding oscillators, as a means of providing insights into the response of more complex engineered systems, such as buildings or bridges. Although this type of simplification was initially motivated by the lack of computational resources for performing dynamic analysis of larger numerical models, in recent years the trend remains - only for different reasons. Advances in performance-based earthquake engineering (PBEE, e.g., [10]) and seismic structural reliability (e.g., [45]) have brought forth the need for an adequate probabilistic representation of structures' post-elastic behavior during earthquake excitation. Due to the inherently stochastic nature of this phenomenon, mainly (but not solely) attributable to the so-called *record-to-record variability* of seismic response [51], such a probabilistic description by analytical means may require a prodigious number of dynamic analyses, putting a strain even on modern computational power. For this reason, methods that employ SDOF-level

approximations of structural systems have been duly preserved in the arsenal of PBEE and have continued to undergo refinement and development.

Looking back, the dynamic response of yielding SDOF oscillators to base acceleration has been in the limelight of earthquake engineering research since its early steps [59] and remained there throughout its evolution, as simplified methods for seismic assessment and design of buildings appeared that were reliant on pushover analysis to define an equivalent, substitute SDOF structure [60,12,7,41,13,46,18]. In more recent years, with the PBEE paradigm gaining an ever-steadier foothold in the earthquake engineering community, new SDOF-based procedures began to surface that additionally sought to map the probabilistic distribution of seismic structural response (e.g., [58,16,5]). Other PBEE-related contexts that employed yielding SDOF oscillators as structural proxies, include the direct use of inelastic displacement as a measure of shaking intensity [54] and the critical scrutiny of prevalent ground motion record selection and modification practices for conducting response history analysis of structures [22,31].

\* Corresponding author.

E-mail address: [georgios.baltzopoulos@unina.it](mailto:georgios.baltzopoulos@unina.it) (G. Baltzopoulos).

Some of the issues that permeate all of the aforementioned cases are: the shape of the backbone curve of the SDOF system, the hysteretic law it follows during cyclic loading and the potential presence of strength and/or stiffness cyclic degradation in the hysteresis. The force-displacement relationship describing response to monotonic static loading; i.e., the backbone curve, is typically an idealization of the pushover curve obtained analytically for the corresponding structure. This idealization can be a simple bilinear shape, or it can also include a descending, negative stiffness branch and even a residual strength plateau. The appearance of negative stiffness in a structure's pushover may be due to P- $\Delta$  effects or material strength degradation (often both) and the importance of its representation on the equivalent SDOF's backbone has been strongly advocated by past research [19,1].

With regard to the hysteretic behavior that ought to characterize a substitute SDOF system in order to best represent global response of the corresponding structure, there was a shift in modern practice, from the simple, kinematic hardening rules that saw extensive use in the past, towards phenomenological, evolutionary hysteretic rules (e.g., [20]) that are more representative of real structural behavior. Various proposals exist in the literature in this regard, typically based on experimental data that refer to specific structural typologies: for instance, the studies of Takeda et al. [53] for reinforced concrete, Graziotti et al. [17] for unreinforced masonry and Lignos and Krawinkler [33] for steel structures, are mentioned. Typically, the same model used for a structure's numerical simulation at the element level (especially in cases of concentrated plasticity modelling) is also assigned to the equivalent SDOF oscillator for that structure. However, it should be noted that, in the case of parametric phenomenological modelling of cyclic degradation effects, experimental model calibration at the element level may not be adequately representative of the entire structure's global behavior and a dedicated study may be needed (e.g., [27]).

The present article introduces a new earthquake-engineering-oriented software: DYANAS, a MATHEMATICS MATLAB®-based graphical user interface (GUI) that expedites the definition of inelastic SDOF systems in the OpenSees (Open System for Earthquake Engineering Simulation; [40]) finite element platform, streamlines the execution of dynamic analyses under suites of base-acceleration time histories and allows for methodical processing of the final results. The analysis method and post-processing aspects of the software are focused on facilitating dynamic analysis schemes that draw on the PBEE paradigm. The graphical interface components of the software run in MATLAB environment. Interaction with OpenSees is performed by manipulating Tcl/Tk scripts (Tool Command Language – a general scripting language that has been extended with OpenSees-specific commands; [42]) via MATLAB functions, in a process that will be described in the following sections.

OpenSees is an open-source, object-oriented finite element platform developed for PBEE. Since its inception, OpenSees has seen extensive use for numerical analysis in structural, geotechnical and seismic reliability problems (e.g., [50]). In the past, various GUIs have been built around OpenSees, intended to facilitate the definition of numerical models and subsequent running of analyses. Such examples are the Build-X software [47] and the GID interface [43] that are both intended for aiding the definition of multi-DOF building models, as well as the web platform of Dolšek et al. [11] and the II-DAP interactive interface [32] that operate on the SDOF level. DYANAS is a new addition to this list and is, primarily, a PBEE tool that incorporates a multitude of functions oriented towards efficient seismic analysis of simple structures (e.g., [56]).

The software presented in this article, DYANAS, is freely available for research purposes as a software package ([http://wpage.unina.it/georgios.baltzopoulos/software/software\\_page.html](http://wpage.unina.it/georgios.baltzopoulos/software/software_page.html)) and is also distributed as open-source code, obtainable at <https://github.com/georgebaltz/SDOF-OSEES>. DYANAS allows users to easily define yielding SDOF oscillators with classical viscous damping, piece-wise linear monotonic backbones and a choice of six evolutionary or

hardening hysteretic rules that are already implemented in OpenSees (to follow). Subsequently, the GUI gives users the opportunity to perform non-linear dynamic analyses to large sets of accelerometric input, supporting incremental dynamic analysis (IDA; [55]), multiple-stripe analysis (MSA; e.g., [25]) and cloud analysis (e.g., [26]). For each analysis session, users may define a single, or two uncoupled, SDOF oscillators. In the latter case, these can be run simultaneously, using bidirectional ground motion records. Finally, the software has the capability to post-process results, graphically represent them for the users and allows exporting figures and data files for further elaboration. The remainder of this paper is organized in the following fashion: first, an outline of the dynamic analysis methods prevalent in PBEE and supported by the GUI is given. Subsequently, a description of the software's function, structure and capabilities is provided. Then, a section dedicated to a few illustrative applications that showcase specific aspects of the software's utility as a PBEE tool are to be found, followed by some closing remarks and discussion.

## 2. Dynamic analysis methods for PBEE

The primary use of dynamic structural analysis in PBEE is as a means of quantifying the ability of a structure to meet certain performance objectives, in a probabilistic framework. An understanding of this can be obtained through Eq. (1), that looks at part of the PEER framing equation [8] to provide the annual rate of a structure's failure to meet some performance objective,  $\lambda_f$ , which is a measure of seismic risk.

$$\lambda_f = \int_{im} P[EDP > edp_f | IM = im] \cdot d\lambda_{im} \quad (1)$$

Eq. (1) is based on two fundamental variables, the so-called engineering demand parameter (EDP) and the seismic intensity measure (IM) that will be both assumed scalar, for simplicity. In that case,  $\lambda_{im}$  represents the annual rate of exceeding a specific value  $im$  at the site of the structure and is therefore a measure of seismic hazard [39]. Finally, the conditional probability that structural response given a certain IM level, exceeds the performance objective threshold,  $edp_f$ ,  $P[EDP > edp_f | IM = im]$  is typically termed a fragility function (sometimes simply written as the probability of failure given IM,  $P[f | IM = im]$ ). EDP is a generic term used for any measure of structural response of engineering significance, that can be used to check or determine if the structure has failed to meet a given performance objective due to, for example, excessive stress or deformation. Examples of often-used EDPs for building structures are inter-storey drift ratio or roof-level displacement. In this context, failure (sometimes also termed “exceedance of a limit state”) can be expressed as the exceedance of a predefined threshold EDP-value. On the other hand, an IM can be some direct instrumental measure of ground motion amplitude, such as peak ground acceleration (PGA), or a quantity of elastic response, such as spectral pseudo-acceleration at various periods,  $S_a(T)$ .

While the concept of structure-specific fragility functions sees extensive use in PBEE and seismic risk analysis, in order to determine such a functional relationship between EDP and IM as  $P[EDP > edp_f | IM = im]$  by analytical means, engineers may need to resort to a number of nonlinear dynamic analyses of a numerical model of the structure, according to some methodology that maps the distribution of EDP for various IM levels. The methods used most frequently to obtain this EDP-IM mapping for seismic response are incremental dynamic analysis, multiple-stripe analysis and cloud analysis. The principal objective of this software is to streamline and facilitate the execution of these types analyses using suites of ground acceleration records, when the structural model adopted is an SDOF simplification of the original structure (or an actual SDOF system, naturally). For this reason, the three aforementioned dynamic analysis methodologies (plus a variant of IDA) are briefly outlined below, whilst other issues mentioned in this first part of the section, such as seismic fragility and

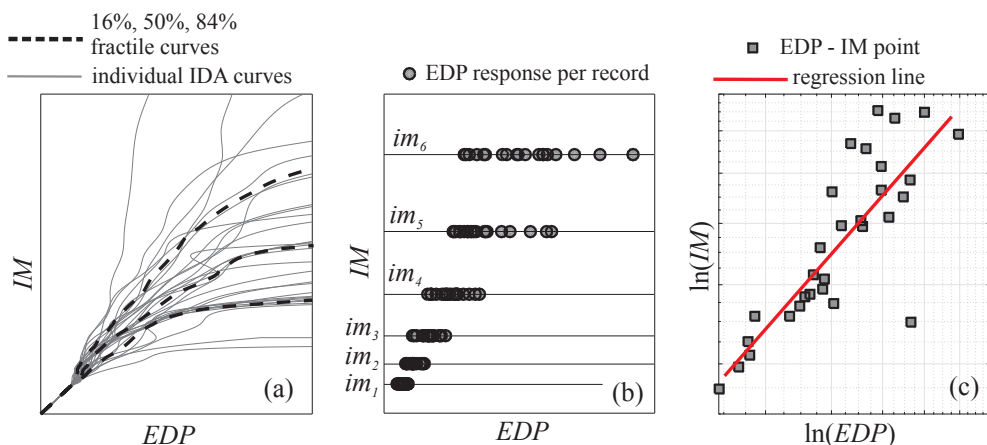


Fig. 1. Illustrating the dynamic analysis methods most frequently used in PBEE: thirty IDA curves of a yielding SDOF oscillator and corresponding 16, 50, 84% EDP-given-IM fractile curves (a); EDP responses of a non-linear structure at six IM levels obtained via MSA (b); logarithmic-scale scatter plot of EDP-IM responses obtained via cloud analysis and corresponding ordinary least squares regression line (c).

hazard will receive little more attention, by virtue of being beyond the scope of the software presented.

2.1. Incremental dynamic analysis

IDA consists of running a series of dynamic analyses for a non-linear structure, using a suite of accelerograms that are progressively scaled upwards in amplitude in order to represent a broad range of IM levels. Structural response, in terms of some EDP, is being continuously registered at each IM level; thus, for each acceleration record, a continuous EDP-IM relationship is obtained, termed an IDA curve (Fig. 1a). A common way of summarizing IDA results for the entire suite of records, is to calculate the 16, 50 and 84% fractile IDA curves of EDP given IM or vice-versa. As can be seen in the figure, while individual-record IDA curves can be non-monotonic, the fractile curves generally are. In fact, for structures susceptible to dynamic instability, when a record is scaled up to levels that can induce such behavior, the IDA curve tends to become horizontal, indicating almost-infinite increase in EDP for small IM increments; thus IDA flat-lines are taken to indicate structural collapse (for further details the interested reader is referred to [55]). It is mentioned in passing that IDA has already found its way into guidelines for practicing engineers that espouse PBEE principles (e.g., [15]).

2.2. Multiple-stripe analysis

MSA, like IDA, has the objective of calculating EDP-responses of a structure at various, increasing IM levels. The difference from IDA is that MSA does not necessarily resort to scaling the same suite of accelerograms to reach these IM levels, but may instead use different sets of (scaled or unscaled) records at each IM level (e.g., [25]). Ideally, these record sets should be selected to reflect site-specific seismic hazard at each IM level, thus rendering the calculated seismic structural demand hazard-consistent (e.g., [34]). A schematic example of MSA results is given in Fig. 1b, where it can be seen that EDP response samples, sometimes termed “EDP-stripes”, have been obtained for six IM levels (note that in the context of IDA and due to the continuous nature of IDA curves, apart from EDP-given-IM, one may also calculate “IM-stripes” for a given EDP value).

2.3. Cloud analysis

Cloud analysis gets its name from the fact that it uses sets of unscaled acceleration records, meaning that, typically, only a single record will correspond to each IM level (besides it being not-very-likely to find many records with, say, the exact same PGA or Sa(T) value, the very nature of this method calls for an even spread of intensity values within the range of interest). This results in a “cloud” of points in the

EDP-IM plane, such as the scatter-plot shown in Fig. 1c. With the cloud method, a probabilistic relation between EDP and IM can be obtained by means of linear regression and its assumptions of homoscedastic, Gaussian residuals (e.g., [26]). Regression of cloud analysis EDP-IM data can find application in some simplified seismic reliability methods; the interested reader is referred to Cornell et al. [9] for further details.

2.4. Back-to-back incremental dynamic analysis

Besides traditional IDA, an extended version thereof has also been suggested in the past [37]. This extension of IDA was intended to provide a probabilistic description of seismic response for structures that have already been damaged by a mainshock earthquake (MS) and are susceptible to the effect of aftershocks (AS) before any repairs can take place. In this type of analysis, henceforth referred to as *back-to-back IDA*, the analyzed structure is first subjected to an initial set of accelerograms, let us call them the MS record set, each scaled to produce the same predefined EDP level. At the end of each single-run MS analysis, a damaged incarnation of the structure has been produced; this is allowed to revert to at-rest conditions and is subsequently subjected to a second set of records, let us call these the AS set, that are scaled upwards in the traditional IDA manner. Fig. 2 provides a schematic representation of this procedure. The end result, as in traditional IDA, is a set of continuous EDP-IM curves, the difference being that these curves no longer describe the seismic behavior of the original

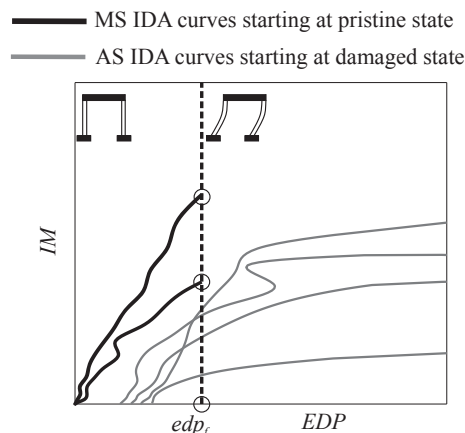


Fig. 2. Schematic representation of back-to-back IDA: a “mainshock” record acting on a structure in pristine condition is scaled until a limit state threshold  $edp_f$  is reached, then IDA is performed for a set of “aftershock” records, acting on the structure damaged by the mainshock record; the procedure is repeated for a predefined number of “mainshock” accelerograms, each followed by a set of “aftershock” accelerograms.

structure, but that of the structure that has been subjected to a specific damaged state. Also note, that the MS-AS characterization of the two record sets employed in this discussion is purely conventional and was used for designating the order with which the two shocks are considered in the analysis, without implying that they must be part of the same seismic sequence.

### 3. Software structure and graphical user interface

DYANAS is structured around two main pillars: the various MATLAB-coded pre- and post-processing tools that are incorporated into the GUI and the suite of parametric scripts that run directly on the OpenSees platform. In order to run an analysis defined by the user via the MATLAB GUI, OpenSees must be provided with Tcl/Tk scripts that contain definition of the numerical model, loading, and the analysis' operational parameters, including what response information to save. These Tcl/Tk scripts are divided into two categories: parametric and definition files. Parametric scripts contain all the information necessary for model definition and execution of analysis in OpenSees, as functions of externally-defined placeholder variables or as hard-coded analysis parameters; these files remain unchanged during any analysis session of the software (unless the user decides to make a direct, outside intervention of course). On the other hand, the definition files are constantly over-written by the GUI's pre-processing tools, according to user input and system definition. Once OpenSees concludes a packet of user-requested analyses, output files are created, that are subsequently parsed by the GUI's post-processing MATLAB routines for further elaboration of the raw results. This procedure is schematically depicted in the flowchart of Fig. 3.

The pre-processing, (system and analysis definition) functionalities of the GUI can be further split into two main groups: definition of the

SDOF system characteristics, such as dynamic properties, backbone curve and the rules governing hysteretic behavior, and definition of the type of analysis, including definition of controlling parameters and handling of dynamic input. The post-processing tools, on the other hand, enable organizing, plotting and extracting specific subsets of the results, in various common formats, useful within the PBEE framework. The remainder of this section describes the salient features of the functionalities outlined above.

#### 3.1. Definition of oscillator characteristics, engineering demand parameter and seismic intensity measure

The first step in any new analysis session is the definition of the system to be analyzed, that may either be an SDOF oscillator or two uncoupled simple oscillators. In the latter case, two separate SDOF systems are defined and analyzed simultaneously, without any interaction occurring between them. This can be useful in the case of regular, symmetrical structures, for which equivalent SDOF systems may be defined via pushover in both principal directions [49].

In all cases, the SDOF system definition requires the assignment of dynamic characteristics, such as period of natural vibration  $T$  and viscous damping ratio  $\nu$  (modelled as mass-proportional), backbone curve and hysteretic rule. The backbone curve corresponds to a piece-wise linear idealization of the force-displacement response of the system to monotonic loading and is defined by the yield strength and displacement,  $F_y$  and  $\delta_y$ , respectively, and up to four parameters for a quadri-linear case, shown in Fig. 4.

These are the hardening slope  $\alpha_h$  (positive ratio of post-yield stiffness to elastic stiffness), the capping-point ductility  $\mu_c$  (point where loss of strength with increasing deformation begins), the post-capping slope  $\alpha_c$  (negative slope corresponding the ratio of the negative post-capping

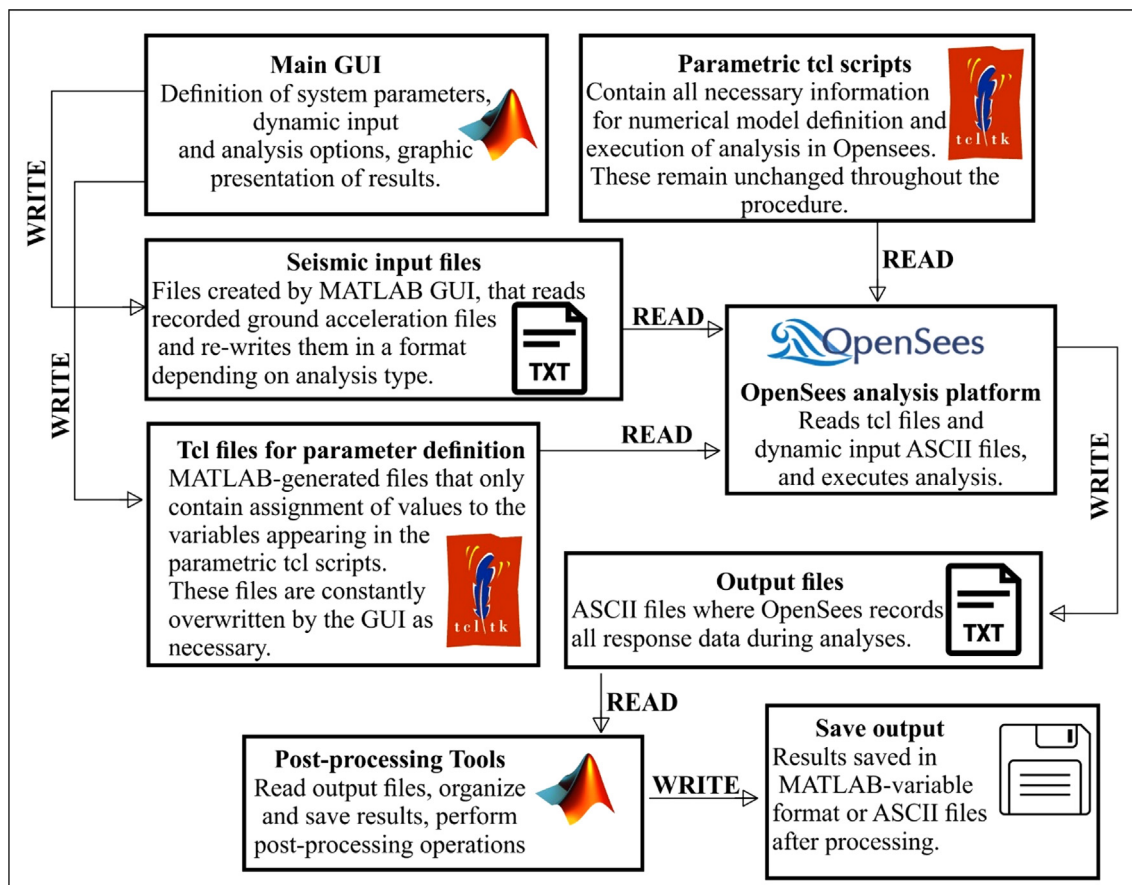


Fig. 3. Operational flowchart of the DYANAS GUI's interaction with OpenSees.



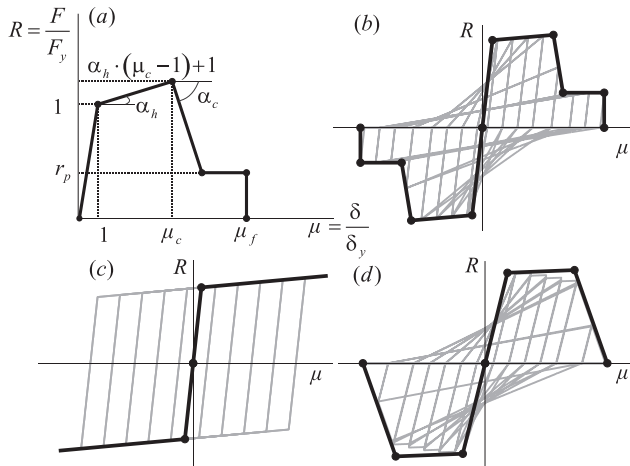


Fig. 4. Definition of non-dimensional parameters for the characterization of an SDOF system's piece-wise linear backbone curve (a); backbone curve with descending branch, residual strength plateau and peak-oriented hysteretic loops (b); bilinear, kinematic hardening system (c); trilinear backbone exhibiting peak-oriented hysteretic behavior with moderate cyclic strength degradation (d).

stiffness divided by the initial elastic stiffness), the height of the residual strength plateau  $r_p$  (ratio of residual strength divided by yield strength) and the fracture ductility  $\mu_f$  (point corresponding to sudden, complete loss of strength), with ductility being response displacement normalized by yield displacement,  $\mu = \delta/\delta_y$ , and strength ratio  $R$  as force normalized by yield strength  $R = F/F_y$ . A sample of the GUI's dialogue windows during the definition of backbone and other properties is provided in Fig. 5.

As can be seen in the figure, the software permits the definition of asymmetric backbone curves, with  $\mu_c$ ,  $\mu_f$  and  $F_y$  being allowed to differ in the two directions, while maintaining the same elastic stiffness. Regarding the choice of hysteretic constitutive law, several options that have been implemented in OpenSees in the past are available [19,20,33,2,35,44]. These are divided into two broad categories of peak-oriented and hardening hysteretic rules and some of them allow for evolutionary behavior, including cyclic strength and stiffness degradation. It should be noted that association of a backbone curve with a descending branch is meaningful only for the peak-oriented hysteretic behavior group; in such cases that include softening branches, in-cycle strength degradation can also emerge during dynamic response (whenever cycles exceed the  $\mu_c$  limit – see also [14]). By means of the “quasi-static cyclic” analysis type, the software offers the user a means to visualize the effect of each hysteretic rule on displacement-controlled cyclic loading.

The second preliminary step, prior to proceeding to the analysis, is to select the EDP and IM that will be employed. For such simple structures as these SDOF oscillators, the choice of EDP is limited to the peak transient displacement in either horizontal direction,  $\delta_x$  and  $\delta_y$ , the residual displacements in both directions and the demand over capacity ratio,  $D/C$ . The  $D/C$  ratio expresses, in non-dimensional form, how close the structure comes to exhausting a threshold EDP. It also provides a means of defining an EDP that takes response in both directions into account, according to the definition in Eq. (2), which is valid for all converging runs, where  $\delta_x^x$  and  $\delta_y^y$  are the “failure” displacements in the corresponding directions (i.e., the EDP thresholds).

$$D/C = \max\{\delta_x/\delta_x^x, \delta_y/\delta_y^y\} \tag{2}$$

Although the actual choice of IM can be deferred until the analysis definition phase (the default option being  $Sa(T)$  at the X-direction

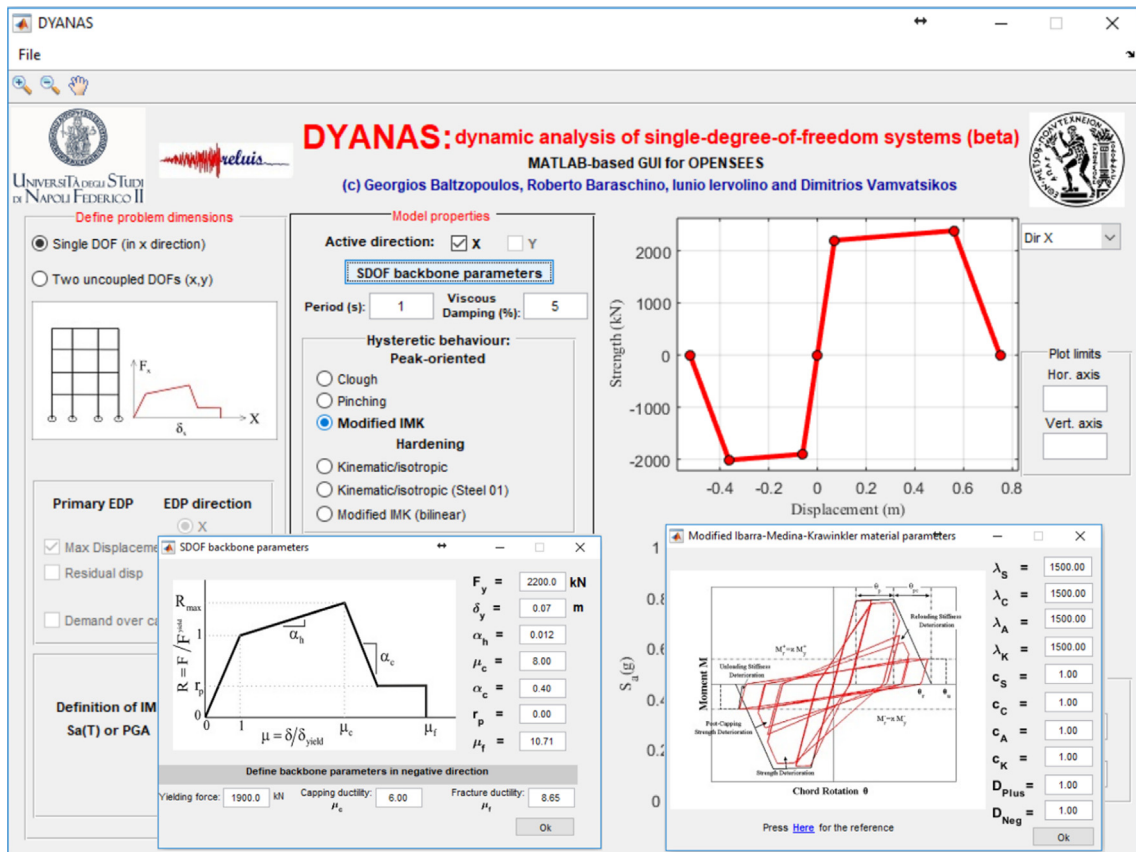
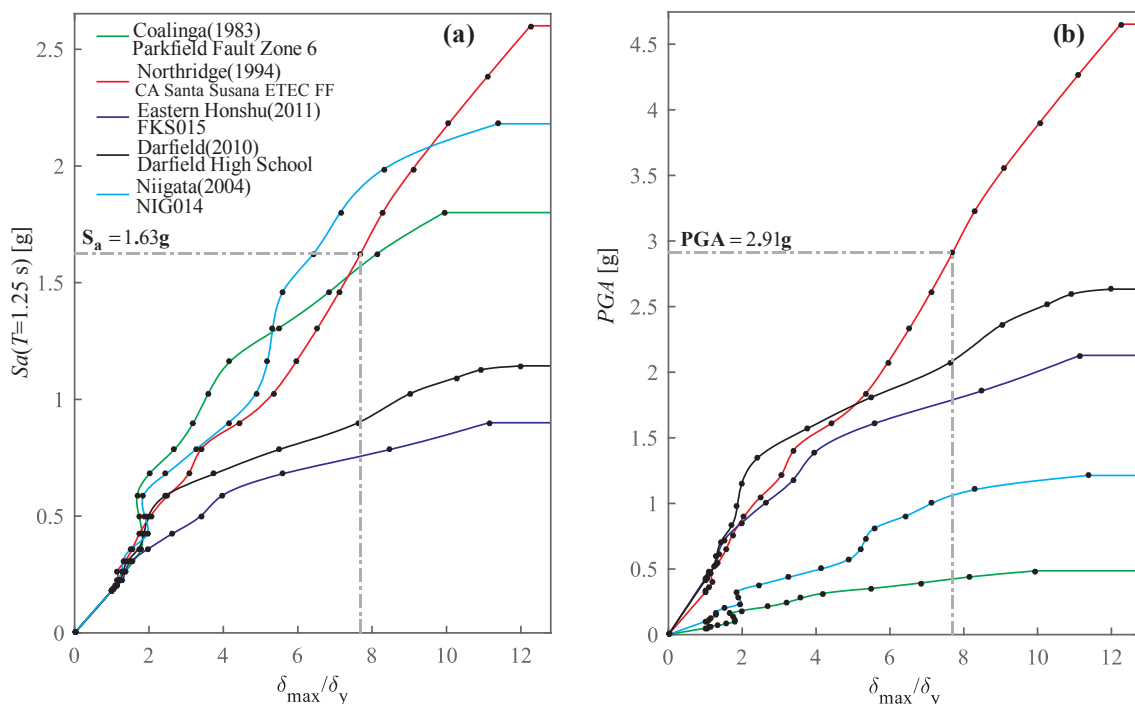


Fig. 5. Main GUI window and subsidiary dialogue windows during definition of a SDOF oscillator's dynamic characteristics, backbone curve (asymmetrical in this case) and hysteretic model.



**Fig. 6.** Conversion of IDA curves from five records between IMs: from  $S_a(T = 1.25\text{ s})$  (a) to PGA (b). The highlighted calculation point on one of the five records used for this example (event, year and recording station reported in the legend) shows the re-mapping of that point between the two panels, the PGA-to-spectral-ordinate ratio for that record being  $2.91/1.63$ . Herein the hunt-and-fill algorithm was stopped prior to evening out the total number of runs per curve, when each flatline was adequately captured.

oscillator's vibration period), in the case of bi-directional ground motion (i.e., definition of two SDOF systems) the user should also determine how that IM is to be calculated: for example,  $S_a(T)$  can be taken as the maximum between the values of the two components,  $S_{a_{\max}}(T)$ , or as the geometric mean of the two,  $S_{a_{gm}}(T)$ .

### 3.2. Running IDA and back-to-back IDA

Due to the particular shape of individual IDA curves, when attempting to adequately represent them by scaling all records at a fixed, constant step in terms of IM, the number of dynamic analyses that may be needed can prove overly time-consuming, even in the case of SDOF systems. DYANAS seeks to optimize required analysis time, by incorporating a MATLAB-programmed implementation of the “hunt-and-fill” algorithm ([56]; [http://users.ntua.gr/divamva/software/bundle\\_runIDA.zip](http://users.ntua.gr/divamva/software/bundle_runIDA.zip)), whereby the number of runs for each record is determined on the fly during analysis. According to this algorithm, after a few test-runs at characteristic IM levels, the software begins to determine the scale factor of the next run based on the history of previous results, resulting on a set of EDP-IM points on the curve – black dots in Fig. 6 – that may be closer or farther apart between curves, in an attempt to use approximately the same number of runs for all curves, regardless of flat-line height. Then, the complete IDA curve (intermediate points – colored segments in Fig. 6) is obtained by means of piece-wise interpolation between these calculation points on the IM-EDP plane ([http://users.ntua.gr/divamva/software/bundle\\_postIDA.zip](http://users.ntua.gr/divamva/software/bundle_postIDA.zip)). Both spline and linear interpolation are possible, with the former being the default option in DYANAS, as it results in smoother IDA curves.

An additional advantage, provided by this computational strategy, is the possibility for nigh-instantaneous change of IM, once a set of IDA curves has been obtained. This IM-change operation can prove useful in a variety of situations, such as when a set of distinct structures must all have their seismic vulnerability functions expressed in a common IM [29] or when the same requirement occurs for the two principal orientations of a single structure [30] or simply for studying the relative

merits of choosing one IM over another [36]. This is also demonstrated in Fig. 6, where the conversion of a set of five IDA curves from spectral pseudo-acceleration,  $S_a(T)$ , at period  $T = 1.25\text{ s}$  to PGA is shown. Given that each explicit calculation point from the trace-IDA implementation, shown in the figure as a black dot upon the spline-interpolated curve, corresponds to a specific scale factor applied to that record, each EDP value at any of these points can be reassigned to the value that the new IM assumes on the record's scaled spectrum. After this re-mapping of the calculation points to the new IM (in this example PGA) is complete, spline interpolation based on the new IM-EDP points provides the converted IDA curves.

The same computational strategy is also followed in the case of back-to-back IDA, with the only difference being in the management/definition of seismic input (to follow). At the conclusion of either of these types of analysis (IDA or back-to-back IDA) a set of post-processing options are available to the user: change of IM or EDP, extraction of IM or EDP stripes that can be saved into MATLAB-variable or text file formats and saving the analysis results for later use. Change of EDP offers a choice between  $\delta_x$ ,  $\delta_y$ , residual displacements and  $D/C$  ratio. Switching EDP is trivial, as all necessary EDP responses are recorded and saved during every single run. Conversion to different IMs, on the other hand, follows the re-interpolation procedure outlined earlier. For single-component ground motion, change of IM entails switching to a spectral ordinate at a different period  $T$  and/or different viscous damping ratio  $\nu$ , with defaults being the X-direction SDOF's period of natural vibration and five percent, respectively. In the case of bidirectional motion, the definition of the IM with respect to the two horizontal acceleration components can also be changed among the already-mentioned alternatives being:  $S_a(T)$  of either single component,  $S_{a_{\max}}(T)$  or  $S_{a_{gm}}(T)$ .

Finally, the post-processing tools of the GUI can provide the extraction of text or MATLAB files containing IDA results organized as either vectors of EDP responses given IM (“EDP stripes”) or IM causing exceedance of a specific EDP value (“IM stripes”). Such output formats may come handy when attempting to fit a parametric probabilistic

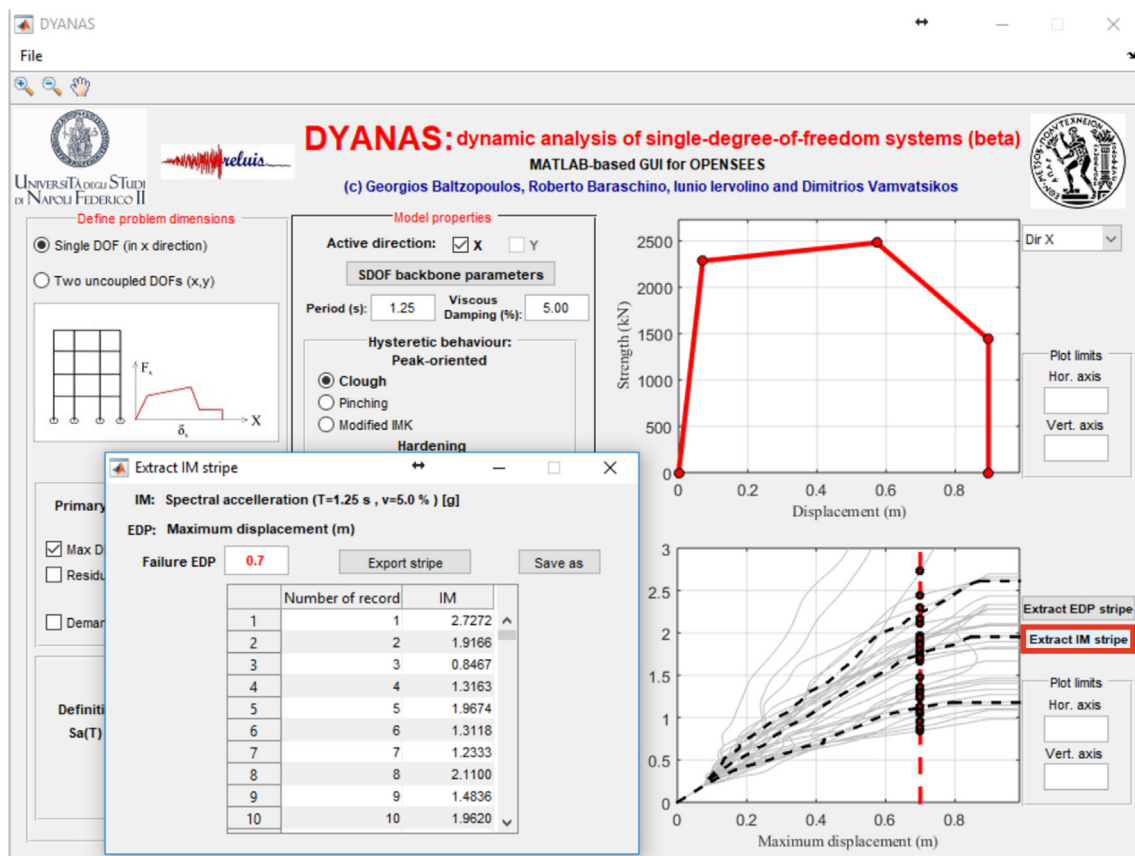


Fig. 7. Extraction of an IM stripe from a set of IDA curves. The EDP threshold is defined in the homonymous dialogue window and the intersections with the curves are displayed in the main GUI lower-right window.

model to a fragility function (the interested reader is referred to [4], for the nuances of fitting such a model in the IM- and EDP-based case). For IM stripe extraction (example provided in Fig. 7), the software finds the intersection of each spline-interpolated IDA curve with the vertical line passing through the user-defined EDP threshold; the lowest IM value is returned in the case of non-monotonic IDA curves that intersect the line at more than one point. For EDP stripes, the user defines a vector of desired IM values and the software returns the intersections with the corresponding horizontal lines; for IDA curves that have already flat-lined below a given IM level, the information that the structure has collapsed is returned.

### 3.3. Running multiple-stripe and cloud analysis

To conduct MSA, the user must define all IM levels for which EDP responses are needed beforehand, via the dedicated dialogue window of the GUI (Fig. 8), and subsequently assign a set of records to each IM stripe. Each stripe must be assigned a specific IM value and all records in the stripe will be then scaled to match that value (exception to that rule is cloud analysis, see below). Internally, analysis is run using the same MATLAB and OpenSees (Tcl/Tk) routines as for IDA, with the difference that record scaling is completely pre-determined at the start of the analysis and a different seismic input file has to be read at each single run. Note that, in the case of MSA, a change of IM requires re-running the analysis from scratch (unlike IDA – see above) while EDP still can be changed at will after completion of the analysis.

In the present GUI application and for reasons of convenience, cloud analysis is also managed via the MSA window, as one may imagine it as a single-record-per-stripe MSA. The user simply has to define a single IM stripe with a nominal intensity value, which is disregarded, and check the “do not scale records” box; in that case the software will

realize that could analysis is in order and will display the results accordingly, as shown in Fig. 8. For both MSA and cloud analysis, EDP stripes can be exported in text- or MATLAB-file format, reducing to IM-EDP pairs in the latter case.

### 3.4. Seismic input

Seismic input can be defined by selecting sets of ASCII files, each containing a recorded acceleration time-history. The software can parse two standard accelerograms formats, namely the Pacific Earthquake Engineering Research NGA database format [3] and the Engineering Strong Motion database format [38]. In either case, the necessary information for running the analyses are extracted/computed from the selected files (units, duration, sampling rate, elastic response spectrum) and passed on to the corresponding MATLAB routines, while the actual accelerometric data are written into temporary files suitable for being read by OpenSees. As an alternative to these standard formats, the user may use simple “.txt” ASCII files that contain a single column of acceleration values and will be inquired by the software to provide units and sampling rate.

The software, at this stage, is distributed equipped with two folders that already contain two sets of accelerograms: one is the suite of thirty single-component records used for calibrating the SPO2IDA tool [58] and the other is the twenty-two bidirectional ground motion “far-field” set of FEMA-P695 [15]. Both record sets consist of accelerograms recorded on firm soil, predominantly during California events of magnitude six or greater.

For IDA or cloud analysis, a single set of records must be selected by the user, while, in the case of MSA, different sets may be assigned to each predefined IM level (stripe), all containing the same number of records. Cloud analysis in particular, is defined via the MSA control

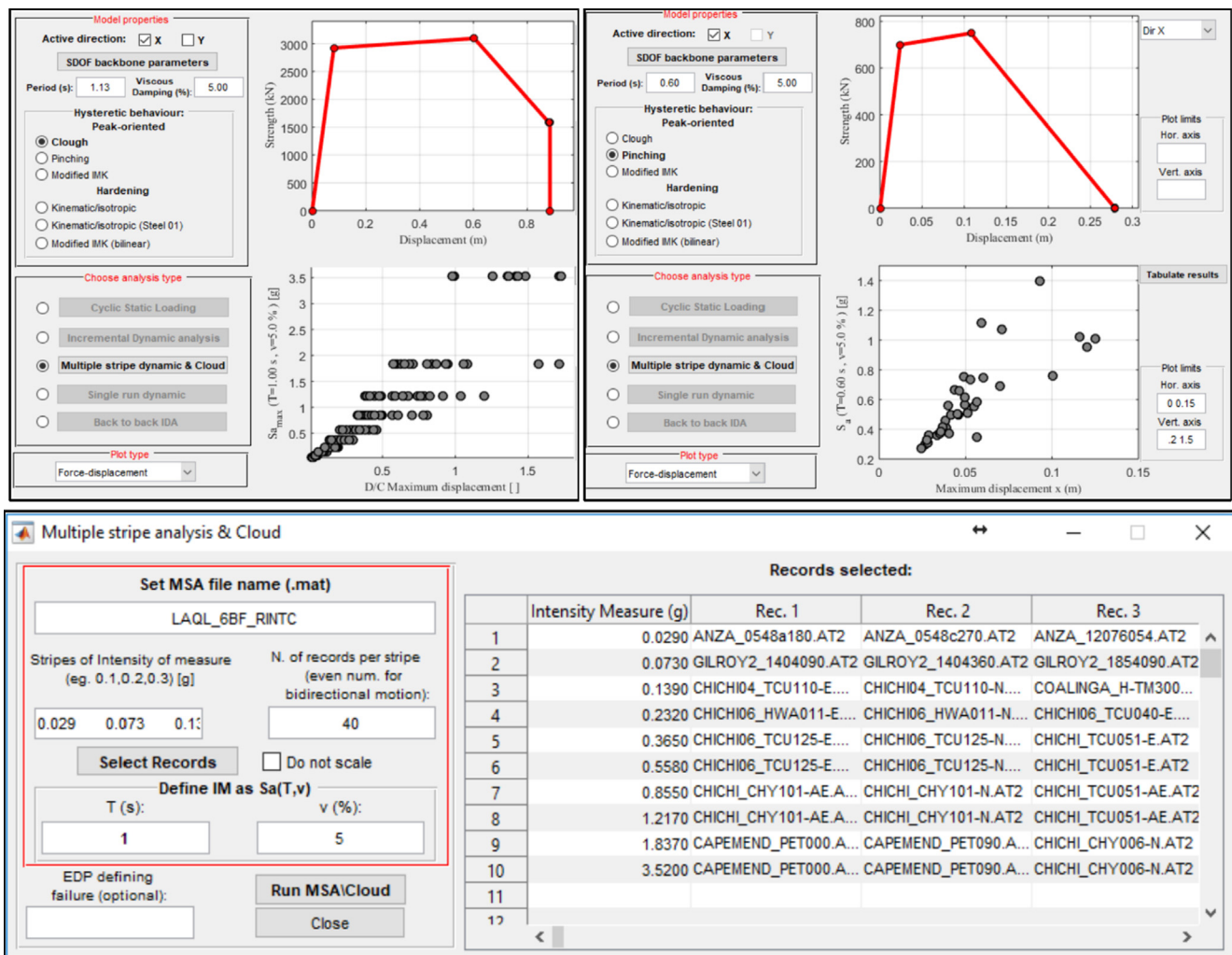


Fig. 8. Main GUI window snapshots displaying the results of MSA (upper left panel) and cloud analysis (upper right panel); MSA dialogue window, showing the setting-up of an analysis at ten levels of seismic intensity (lower panel). All records in each stripe will be scaled to match that stripe's predefined IM level, unless the "Do not scale" checkbox is ticked, in which case cloud analysis runs.

panel, by suspending record scaling, as discussed above. Back-to-back IDA on the other hand, requires two sets of records: the first set, referred to as the MS set, is used to perform a preliminary IDA analysis, that serves to determine the scale factors necessary to induce the predefined EDP value, associated with some structural limit state, across the entire MS record set. During any type of analysis, each record is followed by an appendix of zero acceleration entries for a duration of five times the elastic period of the system, intended to provide time for the residual velocity at the end of the excitation to be damped down to negligible values. This is performed internally in OpenSees, without tampering with the records, so that the next shock will find the system at rest. This procedure is implemented to achieve increased precision in the calculation of residual displacements, which is especially important in the case of back-to-back IDA.

The second set of accelerograms, referred to as the AS set, is used to run an IDA that always follows one of the MS records (the user is actually free to use the same set to represent both MS and AS if one so desires, or two sets of different size). In other words, each scaled AS record acts on a structure that has already experienced the predefined transient maximum EDP value and has had some time to come to quasi-rest conditions. In Fig. 9 the analysis-parameter definition panel for back-to-back IDA is shown, with the AS acceleration-file selection-window open. The user is additionally given the option to define the number of AS IDAs that are going to be run per MS record, ranging from

one to the number of records in the AS set. When the number of IDAs requested per MS is less than the number of AS accelerograms defined, a random extraction is performed from among the AS records (independent extractions are performed for each MS record). A final option available to the user for back-to-back IDA, is that one may request that all MS-AS pairs be created so that no AS record is ever used twice, provided that an adequate number of records has been provided.

In the case of bidirectional ground motion, record assignment proceeds as in the single-component-of-motion case, with the difference that all record sets must be even in number, so that they may be divided in two halves and re-assigned to each of the two directions. Pairing of the records follows the ASCII dictionary alphabetical order of the filenames, by assigning any two consecutive records first in the X and then the Y direction. This is intended to take advantage of the fact that, in most strong ground motion databases, accelerograms recorded by two streams of the same station will be typically saved under filenames differing by only a few characters.

#### 4. Illustrative applications

In this section, some applications are provided as examples, in order to illustrate DYANAS' functionality in more practical terms. The first example uses a pair of relatively regular and symmetrical buildings, for which equivalent SDOF structures are considered in each principal



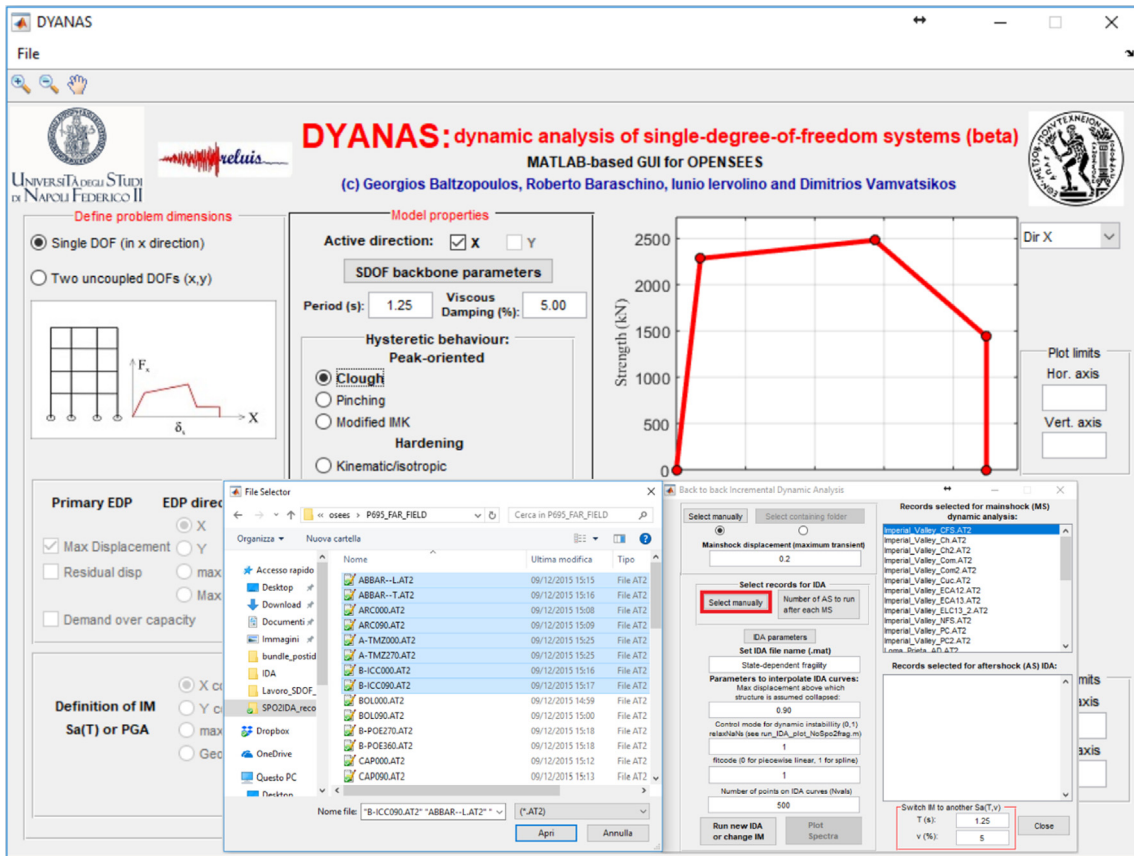


Fig. 9. Selection of accelerograms for running back-to-back IDA; the MS record set list has been already filled and the record-selection dialogue window is open for designating the AS set.

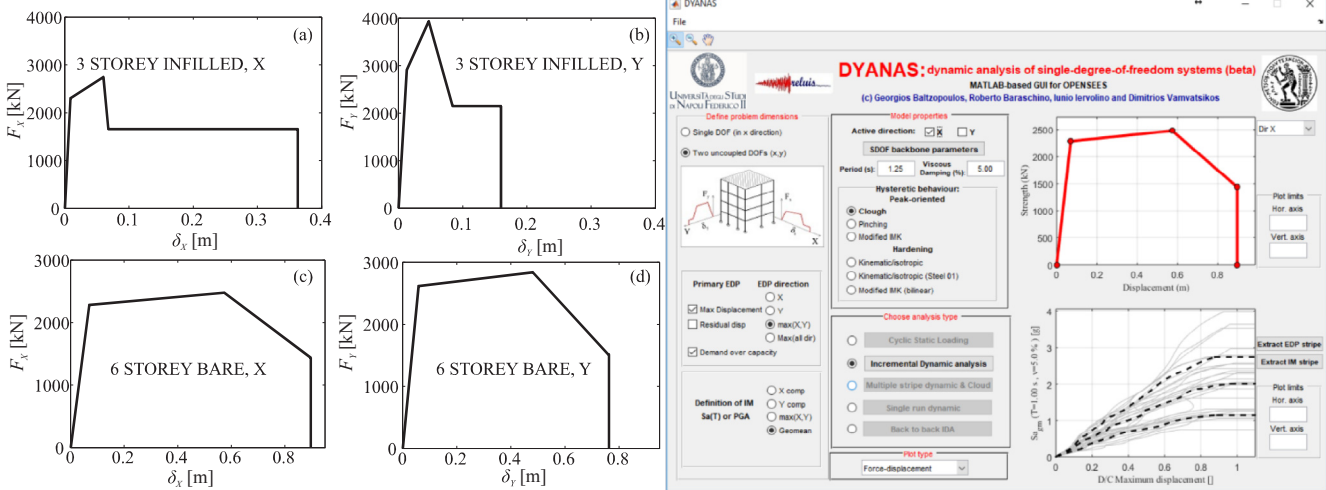


Fig. 10. Piecewise-linear idealizations of the RC frames' static pushovers: three-storey frame with masonry infills, direction X (a) and direction Y (b), six-storey bare frame direction X (c) and direction Y (d). To the right of the pushovers, the GUI main window is shown in post-analysis of the six-storey frame.

direction, to provide applications of IDA and MSA. The second example deals with cloud analysis, while the third application presents the use of back-to-back IDA. In order to consolidate the usefulness of the GUI as a PBEE tool, some of these examples involve the calculation of fragility functions for SDOF structures, based on IDA results. However, it should be clear that the primary scope of the software is to use non-linear dynamic analysis to provide EDP-IM relationships, one natural use of which is the assessment of seismic structural fragility.

#### 4.1. Two equivalent SDOF systems representing both principal directions of a building

For this example application, four static pushovers were used, corresponding to the two principal directions of two code-conforming, reinforced concrete (RC), moment-resisting frame buildings. These two buildings, a three-storey frame with masonry infills and a six-storey bare frame, were designed according to the current Italian seismic code and subsequently numerically modelled [6]. The scope of these numerical models, which were also used to obtain the pushover curves,

was the analytical assessment of seismic collapse risk implicit in the Italian code's provisions, via non-linear dynamic analysis [24]. Considering both buildings in either direction, pushover analysis was performed using a force distribution according to the modal load of each direction's predominant elastic mode shape. Thus, four equivalent SDOF systems with tri- or quadri-linear backbones were derived from these static pushover curves (for further details, see Suzuki et al. [52]) and a Clough-type, peak-oriented model without cyclic deterioration [2], was assumed to govern hysteretic response.

The two equivalent SDOF oscillators corresponding to the three-storey infilled frame had vibration periods of 0.28 and 0.31 s while those of the six-storey bare frame were 1.11 and 1.25 s. As can be seen in Fig. 10, the bare RC frame is characterized by similar maximum attainable base shear and displacement capacity in both directions. On the other hand, the infilled frame exhibits higher maximum resistance in one direction with respect to the other. This is due to the increased presence of openings in the masonry infills along the direction parallel to the building's facade, resulting in lower infill-contribution to lateral strength in that direction. Furthermore, it can be seen that this building is characterized by different ultimate displacement capacity per principal direction.

#### 4.1.1. Incremental dynamic analysis for estimation of collapse fragility

In this exercise, each pair of equivalent SDOF systems, corresponding to a single RC building, was subjected to IDA using a suite of thirty, two-component acceleration records. These accelerograms were recorded on firm soil during events of magnitude ranging from 6.1 to 7.6, at distances from the fault plane 44 km or less and are considered to not exhibit impulsive characteristics due to directivity; during IDA, the same scale factor was applied to both horizontal components with each pair thus always maintaining their as-recorded relative amplitudes. In order to be able to express the seismic collapse fragility of these structures in terms of a common IM, the geometric mean of the two components' spectral acceleration at one second period,  $Sa_{gm}(T = 1.0 \text{ s})$ , was arbitrarily selected and all IDA curves were converted to that IM. For each building three collapse fragility functions were calculated, two curves considering each principal direction  $X$ ,  $Y$  separately and one corresponding to the entire building, i.e., considering both directions at once. In the first two cases, the EDP was set to  $\delta_X$  or  $\delta_Y$  and IM stripes were extracted at  $\delta_f^X$  and  $\delta_f^Y$ , respectively. In the third case, the  $D/C$  ratio according to Eq. (2) was taken as EDP and the IM stripe for  $D/C = 1$  was obtained. It follows from Eq. (2) that, if one were to name failure in the two directions  $f_X$ ,  $f_Y$  and since failure of the entire structure can be seen as the union of the two events,  $P[f | IM = im] = P[f_X \cup f_Y | IM = im] = P[D/C > 1 | IM = im]$ . In all cases, lognormal seismic fragility functions are estimated according to Eq. (3), where  $im_i^f$  represents the  $i$ -th record's (lowest) scaled IM value causing exceedance of the threshold (i.e., the  $i$ -th element of the IM stripe at that threshold, according to the nomenclature used earlier),  $\eta$  and  $\beta$  are the mean and standard deviation, respectively, of the logs of  $im_i^f$ ,  $\Phi(\cdot)$  is the standard Gaussian function and  $n$  is the total number of records.

$$\begin{cases} P[f | IM = im] = \Phi\left[\frac{\ln(im) - \eta}{\beta}\right] \\ \eta = \frac{1}{n} \cdot \sum_{i=1}^n \ln(im_i^f) \\ \beta = \sqrt{\frac{1}{n-1} \cdot \sum_{i=1}^n [\ln(im_i^f) - \eta]^2} \end{cases} \quad (3)$$

The resulting fragility curves are shown in Fig. 11. At this point, it may be useful to recall that the procedure outlined above (as well as those in the following illustrative applications) is inextricably linked to the requisites behind conducting a pushover-based SDOF simplification of a real structure. The main requisites are the predominance of the first mode going into the inelastic response range and that the structure be characterized by sufficient symmetry and regularity for response in the two principal directions to remain largely uncoupled and unaffected by

torsion (e.g., [49]). For this reason, extending evaluations that are based on an equivalent SDOF systems' seismic response, to the actual corresponding multi-DOF structure, may require additional effort to account for the influence of higher modes (see for example [57,28,5]). This being an illustrative example intended to demonstrate the capabilities of this software, with no pretense of using the result for seismic risk assessment of any real structure, considerations need not and will not depart from the SDOF level.

With these premises in mind, it can be seen from the figure that, in the case of the infilled RC frame (Fig. 11a), separate evaluation of collapse fragility along the principal directions results in quite different probability distributions of collapse intensity, with median collapse intensities in the  $X$  and  $Y$  directions being  $\exp(\eta_X) = 1.97 \text{ g}$  and  $\exp(\eta_Y) = 1.19 \text{ g}$ , respectively. In this case of one direction nominally exhibiting greater seismic vulnerability than the other by a wide margin (when the two are viewed as separate structural systems during analysis) it happens that the entire system's collapse fragility almost coincides with the most vulnerable one, with  $\exp(\eta) = 1.17 \text{ g}$ .

On the other hand, in the case of the bare RC frame (Fig. 11b), collapse fragilities derived separately for each direction are more uniform, with  $\exp(\eta_X) = 2.31 \text{ g}$  and  $\exp(\eta_Y) = 2.12 \text{ g}$ . However, in this case, the simplified analysis executed for this example indicates that the total building vulnerability is greater than the worst of the two nominal vulnerabilities obtained by the separate analyses, with a median collapse intensity of  $\exp(\eta) = 1.86 \text{ g}$ .

#### 4.1.2. Multiple-stripe analysis using different sets of records per level of seismic intensity

In this example, a six-storey bare RC frame building is used, designed for a site in L'Aquila, Italy [6]. Details on the equivalent SDOFs in the two principal directions of the structure can be found in Suzuki et al. [52], while the backbone curve in the  $X$  direction is shown in the upper left panel of Fig. 8. In order to calculate site-specific seismic risk for that building, Iervolino et al. [24] selected hazard-consistent sets of records at ten different levels of seismic intensity, when said intensity was expressed in terms of  $Sa_{\max}(T = 1.0 \text{ s})$ . Thus, twenty pairs of bi-directional acceleration time-histories were obtained, for each IM level, and were assigned to an MSA via the GUI (Fig. 8). In this case, definition of IM-type, i.e., maximum-among-horizontal-components spectral acceleration  $Sa_{\max}$ , has to be defined prior to running the analysis, in order to ascertain correct scaling of the records. EDP for the analysis was defined as a  $D/C$  ratio by setting threshold displacements in both directions, corresponding to a roof drift of the actual building of three percent. The resulting EDP vs IM plot from the analysis can be seen in Fig. 12, where the dashed line at  $D/C = 1$  separates the converging runs between those causing failure to the right and those who do not, to the left. Note that in the two highest IM levels,  $Sa_{\max}(T = 1.0 \text{ s}) = 1.837 \text{ g}$  and  $3.52 \text{ g}$ , two and ten cases, respectively, reached collapse and are thus not present on the plot; collapsed cases per stripe are reported separately by the GUI.

#### 4.2. Running cloud analysis via the MSA panel of the GUI

In this brief example application, the trilinear-backbone SDOF oscillator shown in Fig. 13 is used, having vibration period  $T = 0.60 \text{ s}$  and characterized by a moderately-pinched peak-oriented hysteresis [35]. As mentioned previously, in order to run cloud analysis the user has to define a single nominal IM stripe in the MSA panel of the GUI, assign all records to that stripe and select the "do not scale records" option.

For this analysis, a set of forty-two single-component records is selected from within the Engineering Strong Motion database (<http://esm.mi.ingv.it/>), with the criteria of covering a wide range of as-recorded intensity in terms of  $Sa(T = 0.60 \text{ s})$ , never using both components of the same station for a single event, not using more than three stations from the same event and always exceeding yield acceleration of the oscillator in Fig. 13. It is evident that this type of analysis requires a

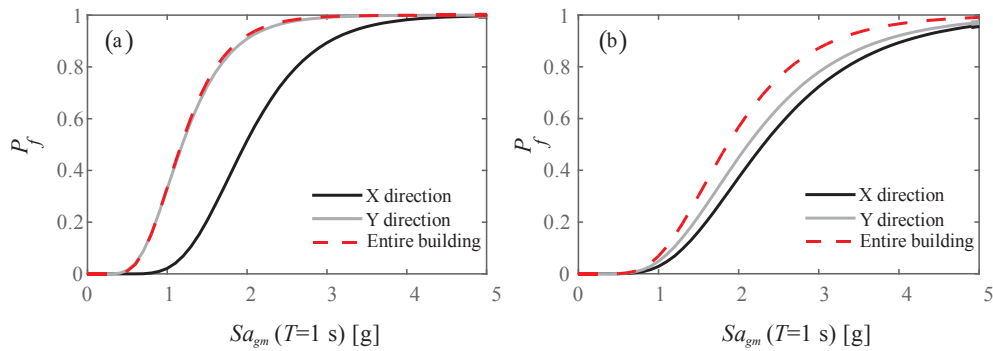


Fig. 11. Collapse fragilities estimated separately for each principal direction and for the entire structure. Fragility curves of the three-storey infilled RC frame (a) and those of the six-storey bare RC frame (b).

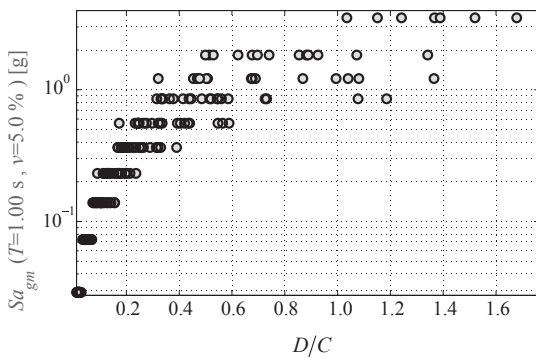


Fig. 12. MSA results shown in a semi-logarithmic EDP-IM plot obtainable via the “export figures” option of the software.

notably lower number of runs with respect to the preceding IDA and MSA examples. The results of the analysis, i.e., an EDP-IM scatter plot forming the homonymous “cloud”, are shown in Fig. 14.

4.3. Back-to-back incremental dynamic analysis for estimating state-dependent seismic fragility

State-dependent seismic fragility extends the traditional concept of fragility, expressed in Eq. (3) as the probability of failure for a given IM level,  $P[f|IM = im]$ , to the probability of failure given both the occurrence of a specific intensity and the structure already being in a generic limit state  $S_i$ ,  $P[f|S_i \cap IM = im]$ . Such state-dependent fragility functions can find application in seismic reliability analysis that considers damage accumulation phenomena (e.g., [23]) and may be analytically estimated by means of back-to-back IDA (see for example [48]).

For this illustrative example, a simple SDOF structure is assumed,

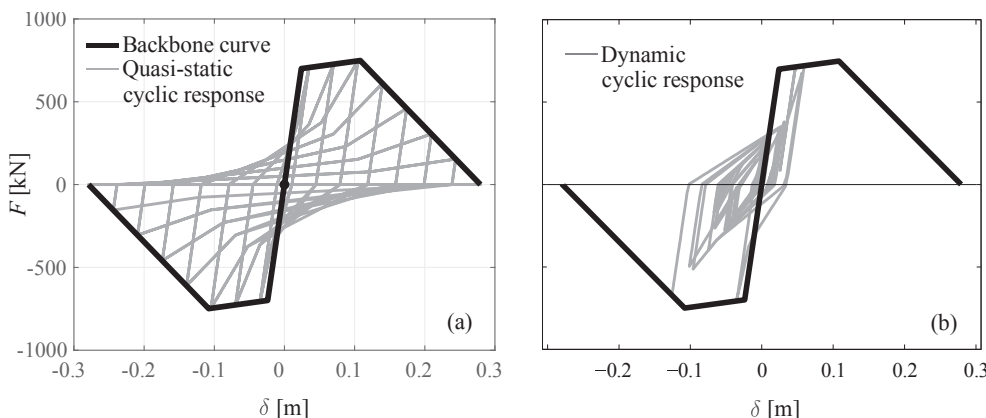


Fig. 13. Trilinear backbone curve of the SDOF oscillator used for cloud analysis and cyclic quasi-static response of the peak-oriented pinched hysteretic model (a); cyclic response of the same to a specific accelerogram (b). Both plots can be obtained via the GUI’s “export figures” option, following a “cyclic quasi-static” or “single-run dynamic” analysis, respectively.

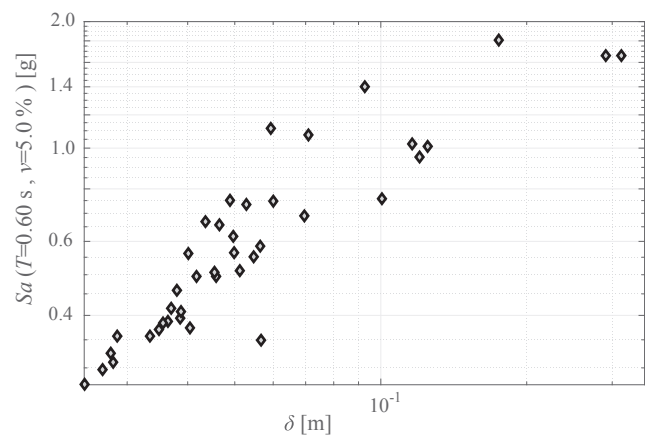


Fig. 14. Results of cloud analysis, shown in a logarithmic-scale EDP-IM scatter plot, obtainable via the “export figures” option of the software.

with vibration period  $T = 0.50$  s and a horizontal post-yield segment stretching up to a capping ductility  $\mu_c = 6.0$ , after which lateral strength drops gradually; hysteresis for this system follows the peak-oriented model of Lignos and Krawinkler [33] and exhibits mild cyclic strength degradation, as shown in Fig. 15. Furthermore, it is assumed that a generic limit state, corresponding to this structure having sustained some seismic damage and indicated as  $S_1$ , is reached when maximum transient seismic ductility demand,  $\mu$ , exceeds 9.6. The example consists of using IDA to estimate the collapse fragility of this SDOF structure at its intact state, indicated as  $S_0$ , and back-to-back IDA for estimating the same fragility under the condition that the structure is in the  $S_1$  state due to one or more prior shocks.

As mentioned in passing earlier, back-to-back IDA is preceded by an IDA performed with a suite of accelerograms designated as the MS set.

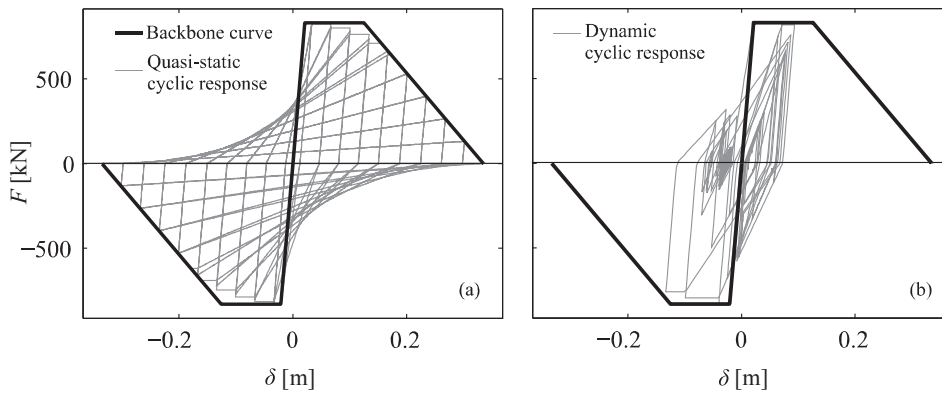


Fig. 15. Backbone curve of the SDOF oscillator used for back-to-back IDA and cyclic quasi-static response of the peak-oriented modified Ibarra-Medina-Krawinkler hysteretic model exhibiting mild strength degradation (a); cyclic response of the same to a specific accelerogram (b). Both plots can be obtained via the GUI’s “export figures” option, following a “cyclic quasi-static” or “single-run dynamic” analysis, respectively.

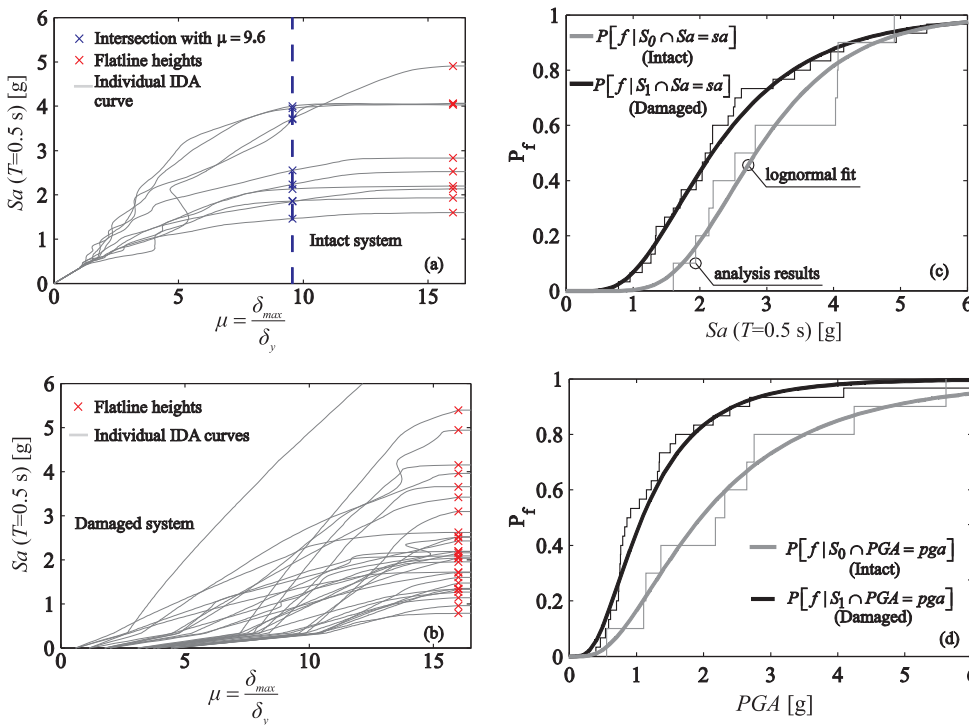


Fig. 16. Preliminary IDA used to determine intact state collapse fragility and intensities inducing the  $S_1$  limit state threshold (a); back-to-back IDA used to determine collapse fragility given that the structure has previously reached the limit state  $S_1$  (b); comparison of collapse fragility curves of the intact and damaged structure, expressed in terms of  $Sa(T = 0.50\text{ s})$  (c) and in terms of PGA (d), after implementation of the IM conversion tool.

In this case, the MS set consisted of ten records and the preliminary analysis provided the scale factors required to reach the  $\mu = 9.6$  threshold that was assumed, by convention, to signify exceedance of  $S_1$  (see Fig. 16a). During back-to-back IDA, each MS record is followed by three AS records that are randomly sampled from within a pool of twenty accelerograms, resulting in thirty curves. For this analysis, the thirty single-component records provided with the software are used. It should be noted that the number of records and back-to-back IDA runs used in this example is simply dictated by the need to maintain Fig. 16 easily legible by avoiding overcrowding of IDA curves. In fact, these numbers should be chosen on the basis of the confidence that the user desires to be able to place on the estimated fragility parameters; the interested reader is referred to Iervolino [21] for more details.

By taking the IM stripes corresponding to the so-called flat-line heights of the IDA curves that, as discussed previously, signify the onset of dynamic instability, collapse fragility curves can be obtained according to Eq. (3) for both  $S_0$  and  $S_1$  initial states. These fragility curves are shown in Fig. 16, in terms of both  $Sa(T = 0.50\text{ s})$  and  $PGA$ , with the latter being derived from the former almost-instantaneously, via re-interpolation of the IDA curves. In either case, one observes the characteristic shift of the  $S_1$  fragilities to the left of the  $S_0$  curves, quantifying the decrease in capacity (or increase in vulnerability) of the structure,

that has befallen a damaged state.

### 5. Concluding remarks

This article was dedicated to the presentation of DYANAS, an open-source, earthquake engineering software. The software is a MATHWORKS MATLAB®-based graphical user interface that interacts with the OpenSees finite element framework and offers engineers an easy way to define and run dynamic analysis of yielding single-degree-of-freedom systems subjected to large suites of earthquake-induced ground motion records. Therefore, the main purpose of this software is to determine the relationship between seismic intensity and engineering demand parameters using any one of several dynamic analysis methods that are frequently used in performance-based earthquake engineering. Incremental dynamic analysis is supported in its traditional form and also in a “back-to-back” format that could allow state-dependent seismic fragility to be estimated. Multiple-stripe and cloud-type analyses are also supported, in cases where the user does not desire to use scaled records to estimate seismic response at different levels of shaking intensity. Much of the software’s utility stems from the post-processing routines, with which it is equipped. These routines, which are also programmed in MATLAB and can be recalled via the user



interface, permit the re-interpolation of incremental dynamic analysis curves, thus providing rapid conversion of the curves into alternative intensity measures, such as peak ground acceleration or spectral ordinates at various periods. Furthermore, at the end of analysis, the user can obtain vectors of intensity measure given engineering demand parameter, or vice versa, thus facilitating further probabilistic seismic demand elaborations for these simple structural systems. Overall, the GUI was shown to be a useful tool within the context of performance-based earthquake engineering, as demonstrated by the illustrative applications provided. DYANAS is freely distributed for research purposes by the University of Naples Federico II under a GNU general public license v3.0, obtainable at <http://wpage.unina.it/georgios.baltzopoulos/software/dyanas.zip>. The MATLAB and Tcl/Tk source code is available at a dedicated GitHub repository at <https://github.com/georgebaltz/SDOF-OSEES>.

## Acknowledgements

The work presented in this paper was partly developed within the activities of ReLUIIS (Rete di Laboratori Universitari d'Ingegneria Sismica) during the 2014-2018 research program, funded by the Italian Civil Protection (DPC – *Dipartimento della Protezione Civile*) - ReLUIIS 2014-2018. Another part of the work was supported via the Horizon 2020 MSKA-RISE research project EXCHANGE-RISK (Experimental & Computational Hybrid Assessment of Natural Gas Pipelines Exposed to Seismic Risk) – Grant no. 691213.

## References

- Adam C, Jäger C. Seismic collapse capacity of basic inelastic structures vulnerable to the P-delta effect. *Earthquake Eng Struct Dyn* 2012;41(4):775–93. <https://doi.org/10.1002/eqe.1157>.
- Altoontash A, Deierlein G. Simulation and damage models for performance assessment of reinforced concrete beam-column joints PhD. Dissertation Department of Civil and Environmental Engineering, Stanford University; 2004.
- Ancheta TD, Darragh RB, Stewart JP, Seyhan E, Silva WJ, Chiou BJS, et al. NGA-West2 database. *Earthquake Spectra* 2014;30(3). <https://doi.org/10.1193/070913EQS197M>.
- Baker JW. Efficient analytical fragility function fitting using dynamic structural analysis. *Earthquake Spectra* 2015;31(1):579–99. <https://doi.org/10.1193/021113EQS025M>.
- Baltzopoulos G, Baraschino R, Iervolino I, Vamvatsikos D. SPO2FRAG: software for seismic fragility assessment based on static pushover. *Bull Earthquake Eng* 2017;15(10). <https://doi.org/10.1007/s10518-017-0145-3>.
- Camata G, Celano F, De Risi MT, Franchin P, Magliulo G, Manfredi V. RINTC project: nonlinear dynamic analyses of Italian code-conforming reinforced concrete buildings for risk of collapse assessment. In: Papadrakakis M, Fragiadakis M, editors. Proceedings of the 6th international conference on computational methods in structural dynamics and earthquake engineering (COMPdyn 2017). Rhodes Island, Greece, 15–17 June. 2017. p. 1474–85.
- Chopra AK, Goel RK. Capacity-demand-diagram methods based on inelastic design spectrum. *Earthquake Spectra* 1999;15(4):637–56. <https://doi.org/10.1193/1.1586065>.
- Cornell CA. Hazard, ground motions and probabilistic assessments for PBSD. In: Fajfar P, Krawinkler H, editors. Proceedings, workshop on performance based design. Bled, Slovenia, June 28–July 1. 2004.
- Cornell CA, Jalayer F, Hamburger RO, Foutch DA. Probabilistic basis for 2000 SAC federal emergency management agency steel moment frame guidelines. *J Struct Eng* 2002;128(4):526–33. [https://doi.org/10.1061/\(ASCE\)0733-9445\(2002\)128:4\(526\)](https://doi.org/10.1061/(ASCE)0733-9445(2002)128:4(526)).
- Cornell CA, Krawinkler H. Progress and challenges in seismic performance assessment. *PEER Center News* 2000;3(2):1–3.
- Dolšek M, Šebenik Ž, Klinc R, Dolenc M, Brozovic M. Web application for the selection of characteristic ground motions. 6th international conference on earthquake geotechnical engineering, Christchurch, New Zealand, 1–4 November. 2015.
- Fajfar P, Gašperšič P. The N2 method for the seismic damage analysis of RC buildings. *Earthquake Eng Struct Dyn* 1996;25(1):31–46. [https://doi.org/10.1002/\(SICI\)1096-9845\(199601\)25:1<31::AID-EQE534>3.0.CO;2-V](https://doi.org/10.1002/(SICI)1096-9845(199601)25:1<31::AID-EQE534>3.0.CO;2-V).
- FEMA. Improvement of nonlinear static seismic analysis procedures. Washington DC: FEMA 440, Federal Emergency Management Agency; 2005.
- FEMA. FEMA P440 – effects of strength and stiffness degradation on seismic response. Washington DC: Fema P440a, Federal Emergency Management Agency; 2009.
- FEMA. Quantification of building seismic performance factors. Washington DC: Fema P695, Federal Emergency Management Agency; 2009.
- Fragiadakis M, Vamvatsikos D. Fast performance uncertainty estimation via push-over and approximate IDA. *Earthquake Eng Struct Dyn* 2010;39(6):683–703. <https://doi.org/10.1002/eqe.965>.
- Graziotti F, Penna A, Magenes G. A nonlinear SDOF model for the simplified evaluation of the displacement demand of low-rise URM buildings. *Bull Earthq Eng* 2016;14(6):1589–612. <https://doi.org/10.1007/s10518-016-9896-5>.
- Guerrini G, Graziotti F, Penna A, Magenes G. Improved evaluation of inelastic displacement demands for short-period masonry structures. *Earthquake Eng Struct Dyn* 2017;46(9):1411–30. <https://doi.org/10.1002/eqe.2862>.
- Ibarra LF, Krawinkler H. Global collapse of frame structures under seismic excitations. PEER Report 2005/06; 2005.
- Ibarra LF, Medina RA, Krawinkler H. Hysteretic models that incorporate strength and stiffness deterioration. *Earthquake Eng Struct Dyn* 2005;34(12):1489–511. <https://doi.org/10.1002/eqe.495>.
- Iervolino I. Assessing uncertainty in estimation of seismic response for PBEE. *Earthquake Eng Struct Dyn* 2017;46(10):1711–23. <https://doi.org/10.1002/eqe.2883>.
- Iervolino I, Cornell CA. Record selection for nonlinear seismic analysis of structures. *Earthquake Spectra* 2005;21(3):685–713. <https://doi.org/10.1193/1.1990199>.
- Iervolino I, Giorgio M, Chioccarelli E. Markovian modeling of seismic damage accumulation. *Earthquake Eng Struct Dyn* 2016;45(3):441–61. <https://doi.org/10.1002/eqe.2668>.
- Iervolino I, Spillatura A, Bazzurro P. RINTC project - assessing the (implicit) seismic risk of code-conforming structures in Italy. In: Papadrakakis M, Fragiadakis M, editors. Proceedings of the 6th international conference on computational methods in structural dynamics and earthquake engineering (COMPdyn 2017). Rhodes Island, Greece, 15–17 June. 2017. p. 1545–57.
- Jalayer F, Cornell CA. Alternative non-linear demand estimation methods for probability-based seismic assessments. *Earthquake Eng Struct Dyn* 2009;38(8):951–72. <https://doi.org/10.1002/eqe.876>.
- Jalayer F, De Risi R, Manfredi G. Bayesian cloud analysis: efficient structural fragility assessment using linear regression. *Bull Earthq Eng* 2015;13(4):1183–203. <https://doi.org/10.1007/s10518-014-9692-z>.
- Kampenhuber D, Adam C. Degradation parameter for equivalent SDOF systems obtained from cyclic pushover analysis and parameter optimisation. Proceedings of the second european conference on earthquake engineering and seismology (2ECEES), Istanbul, Turkey, Aug. 24–29. 2014.
- Kappos AJ, Gkatzogias KI, Gidaris IG. Extension of direct displacement-based design methodology for bridges to account for higher mode effects. *Earthquake Eng Struct Dyn* 2013;42(4):581–602. <https://doi.org/10.1002/eqe.2229>.
- Kazantzi AK, Vamvatsikos D. Intensity measure selection for vulnerability studies of building classes. *Earthquake Eng Struct Dyn* 2015;44(15):2677–94. <https://doi.org/10.1002/eqe.2603>.
- Kohrangi M, Vamvatsikos D, Bazzurro P. Implications of intensity measure selection for seismic loss assessment of 3-D buildings. *Earthquake Spectra* 2016;32(4):2167–89. <https://doi.org/10.1193/112215EQS177M>.
- Kwong NS, Chopra AK, McGuire RK. A framework for the evaluation of ground motion selection and modification procedures. *Earthquake Eng Struct Dyn* 2015;44(5):795–815. <https://doi.org/10.1002/eqe.2502>.
- Elkady A, Lignos DG. Interactive Interface for Dynamic Analysis Procedures (II-DAP): Version 1.0 manual and examples. Switzerland: Resilient Steel Structures Laboratory, School of Architecture, Civil and Environmental Engineering, Swiss Federal Institute of Technology in Lausanne (EPFL); 2018.
- Lignos DG, Krawinkler H. Deterioration modeling of steel components in support of collapse prediction of steel moment frames under earthquake loading. *J Struct Eng* 2011;137(11):1291–302. [https://doi.org/10.1061/\(ASCE\)ST.1943-541X.0000376](https://doi.org/10.1061/(ASCE)ST.1943-541X.0000376).
- Lin T, Haselton CB, Baker JW. Conditional spectrum-based ground motion selection. Part I: hazard consistency for risk-based assessments. *Earthquake Eng Struct Dyn* 2013;42(12):1847–65. <https://doi.org/10.1002/eqe.2301>.
- Lowes L, Mitra N, Altoontash A. A beam-column joint model for simulating the earthquake response of reinforced concrete frames a beam-column joint model for simulating the earthquake response of reinforced concrete frames. PEER Report 2003/10; 2004.
- Luco N, Cornell CA. Structure-specific scalar intensity measures for near-source and ordinary earthquake ground motions. *Earthquake Spectra* 2007;23(2):357–92. <https://doi.org/10.1193/1.2723158>.
- Luco N, Bazzurro P, Cornell CA. Dynamic versus static computation of the residual capacity of a mainshock-damaged building to withstand an aftershock. 13th world conference on earthquake engineering, Vancouver, B.C., Canada August 1–6. 2004.
- Luzi L, Puglia R, Russo E, ORFEUS WG5. Engineering strong motion database, version 1.0. Istituto Nazionale di Geofisica e Vulcanologia, Observatories & Research Facilities for European Seismology; 2016. <https://doi.org/10.13127/ESM>.
- McGuire RK. Probabilistic seismic hazard analysis and design earthquakes: closing the loop. *Bull Seismol Soc Am* 1995;85(5):1275–84. [https://doi.org/10.1016/0148-9062\(96\)83355-9](https://doi.org/10.1016/0148-9062(96)83355-9).
- McKenna F. OpenSees: a framework for earthquake engineering simulation. *Comput Sci Eng* 2011;13(4):58–66. <https://doi.org/10.1109/MCSE.2011.66>.
- Miranda E. Estimation of inelastic deformation demands of SDOF systems. *J Struct Eng (ASCE)*. 2001;127(9):1005–12. [https://doi.org/10.1061/\(ASCE\)0733-9445\(2001\)127:9\(1005\)](https://doi.org/10.1061/(ASCE)0733-9445(2001)127:9(1005)).
- Ousterhout JK, Jones K. Tcl and the Tk Toolkit. 2nd ed. Addison Wesley; 2009.
- Papanikolaou VK, Kartalis-Kaounis T, Protopapadakis VK, Papadopoulos T. GiD + OpenSees interface: an integrated finite element analysis platform. Greece: Lab R/C and Masonry Structures, Aristotle University of Thessaloniki; 2017.
- Perzyna P. Thermodynamic theory of viscoplasticity. (C):313–54. *Adv Appl Mech* 1971;11. [https://doi.org/10.1016/S0065-2156\(08\)70345-4](https://doi.org/10.1016/S0065-2156(08)70345-4).
- Pinto PE, Giannini R, Franchin P. Seismic reliability analysis of structures. Pavia: IUSS Press; 2004.

- [46] Priestley MJN, Calvi GM, Kowalsky MJ. Displacement-based seismic design of structures. Pavia: IUSS Press; 2007.
- [47] Psyrras NK, Sextos AG. Build-X: expert system for seismic analysis and assessment of 3D buildings using OpenSees. *Adv Eng Softw* 2018;116:23–35. <https://doi.org/10.1016/j.advengsoft.2017.11.007>.
- [48] Raghunandan M, Liel AB, Luco N. Aftershock collapse vulnerability assessment of reinforced concrete frame structures. *Earthquake Eng Struct Dyn* 2015;44(3):419–39. <https://doi.org/10.1002/eqe.2478>.
- [49] Seneviratna GDPK, Krawinkler H. Evaluation of inelastic MDOF effects for seismic design PhD. Dissertation Department of Civil and Environmental Engineering, Stanford University; 1997.
- [50] M. Scott T. Haukaas 2006 Modules in OpenSees for the next generation of performance-based engineering Structures congress 2006, 17th analysis and computation specialty conference, May 18–21, St. Louis, Missouri [https://doi.org/doi:10.1061/40878\(202\)33](https://doi.org/doi:10.1061/40878(202)33).
- [51] Shome N, Cornell CA. Probabilistic seismic demand analysis of nonlinear structures. Reliability of marine structures program technical report RMS-35. Stanford University; 1999.
- [52] Suzuki A, Baltzopoulos G, Iervolino I, the RINTC WP4 workgroup (Franchin P, Magliulo G, Masi A, Mollaioli F, Spacone E, Verderame G.). A Look at the seismic risk of Italian code-conforming RC buildings. In: Proc. of 16th European conference on earthquake engineering, Thessaloniki, Greece; 2018.
- [53] Takeda T, Sozen MA, Nielsen NN. Reinforced concrete response to simulated earthquakes. *J Struct Div (ASCE)* 1970;12(96):2557–73.
- [54] Tothong P, Cornell CA. An empirical ground-motion attenuation relation for inelastic spectral displacement. *Bull Seismol Soc Am* 2006;96(6):2146–64. <https://doi.org/10.1785/0120060018>.
- [55] Vamvatsikos D, Cornell CA. Incremental dynamic analysis. *Earthquake Eng Struct Dyn* 2002;31(3):491–514. <https://doi.org/10.1002/eqe.141>.
- [56] Vamvatsikos D, Cornell CA. Applied incremental dynamic analysis. *Earthquake Spectra* 2004;20(2):523–53. <https://doi.org/10.1193/1.1737737>.
- [57] Vamvatsikos D, Cornell CA. Direct estimation of seismic demand and capacity of multidegree-of-freedom systems through incremental dynamic analysis of single degree of freedom approximation. *J Struct Eng* 2005;131(4):589–99. [https://doi.org/10.1061/\(ASCE\)0733-9445\(2005\)131:4\(589\)](https://doi.org/10.1061/(ASCE)0733-9445(2005)131:4(589)).
- [58] Vamvatsikos D, Cornell CA. Direct estimation of the seismic demand and capacity of oscillators with multi-linear static pushovers through IDA. *Earthquake Eng Struct Dyn* 2006;35(9):1097–117. <https://doi.org/10.1002/eqe.573>.
- [59] Veletsos AS, Newmark NM, Chelapati CV. Deformation spectra for elastic and elastoplastic systems subjected to ground shock and earthquake motions. *Proceedings of the world conference on earthquake engineering*. 1965. p. 663–82.
- [60] Vidic T, Fajfar P, Fischinger M. Consistent inelastic design spectra: strength and displacement. *Earthquake Eng Struct Dyn* 1994;23(5):507–21. <https://doi.org/10.1002/eqe.4290230504>.